Natural Convection of Temperature-Sensitive Magnetic Fluids in Porous Media

Valentin Roussellet[1,2], Xiaodong Niu[2,*], Hiroshi Yamaguchi[2], and Frédéric Magoulés[1]

[1] *Applied Mathematics and Systems Laboratory, École Centrale Paris, 92295 Châtenay-Malabry, France*
[2] *Department of Mechanical Engineering, Doshisha University, Kyoto 610-0321, Japan*

Abstract. In this article, natural convection of a temperature-sensitive magnetic fluid in a porous media is studied numerically by using lattice Boltzmann method. Results show that the heat transfer decreases when the ball numbers increase. When the magnetic field is increased, the heat transfer is enhanced; however the average wall Nusselt number increases at small ball numbers but decreases at large ball numbers due to the induced flow being more likely confined near the bottom walls with a high number of obstacles.

1 Introduction

Ferrofluids are a mixture of ferromagnetic nanoparticles in suspension in a carrier fluid [1] which makes them reactive to the presence of a magnetic field. The ferrous particles are usually coated with a surfactant, which allows the suspension to remain in a stable state. Among these fluids, temperature-sensitive magnetic fluids (TSMF) have their magnetization strongly dependent of the temperature [2]. Thus, with properties such as energy transfers and flow which can be controlled with a magnetic field, TSMF have various promising applications, ranging from heat transfer technologies [3,4] to spatial engineering [5], and have been the subject of many researches

---

*Corresponding author.
URL: http://kenkyudb.doshisha.ac.jp/rd/search/researcher/108197/index-j.html
Email: louen@via.ecp.fr (V. Roussellet), xniu@mail.doshisha.ac.jp (X. D. Niu), hyamaguc@mail.doshisha.ac.jp (H. Yamaguchi), frederic.magoules@hotmail.com (F. Magoulés)

during the past years [6–10]. Finlayson [6] first studied thermomagnetic convection of the TSMF and showed the existence of a critical parameter beyond which the thermomagnetic convection occurs. Schwab et al. [7] conducted an experimental investigation of the convective instability in a horizontal layer of the TSMF and characterized influences of the magnetic Rayleigh number on the Nusselt number. Krakov and Nikiforov [8] addressed influences of the relative orientation of the temperature gradient and magnetic field on thermomagnetic convection in a square cavity. Yamaguchi et al. [9, 10] performed experiments and numerical analyses in a square enclosure and characterized the heat transfer in terms of a magnetic Rayleigh number.

However, the behaviors of TMSF still lack studies in cases such as natural convection in porous media, though many practical situations involve a porous structure. Porous media flows have themselves a wide application, from sand filters to petroleum engineering and hydrogeology [11, 12]; therefore the understanding of the magnetic fluid flow in such media could yield useful applications. In the following, we will discuss the results of the numerical simulations of natural convection of TSMF in a porous cavity. To ensure accurate and fast calculations for the complicated magnetohydrodynamics equations in such cases, we used the lattice Boltzmann Method (LBM), a recently developed computational fluid dynamics (CFD) technique [13]. While conventional CFD methods use finite differences or volumes to discretize the continuous fluid dynamics equations, LBM emerges from the Boltzmann equation (BE), and describes the fluid dynamics by means of a density distribution in virtual mesoscopic-scale particles placed along a 2- or 3-dimensional regular lattice. Since then, efforts have been made to extend the basic lattice Boltzmann model to include effects such as heat transfer and convection, or magnetic influence in ferrofluids [14, 15]. For this study of thermal effects in magnetic fluids, the LBM for TMSF described in [15] has been successfully implemented in modeling the ordinary porous flow phenomena. The porous media itself is modeled by different sizes and numbers of spherical obstacles evenly spread across the cavity. The purpose of the present study is to study the effect of the magnetic field to the heat transfer characteristics of flows in the porous media, which is a prototype of a cooling system with porous structure adjacent to the heating wall.

The rest of the paper is organized as follows: in Section 2 we will discuss the methodology of the study, and in particular, the details of lattice Boltzmann method used for the simulation; Section 3 focuses on the results obtained and their explanation. Finally, a conclusion is given in Section 4.

2   Methodology and numerical simulation

2.1   Lattice Boltzmann models

In the theory of the magnetic fluids, as the flow under influences of the magnetic field, it undergoes magnetic force. The magnetic hydrodynamics for the non-conductive magnetic fluid in porous media can be described by the following governing equa-

tions [1,2]

$$\partial_t \rho + \nabla \rho_0 \mathbf{u} = 0, \tag{2.1a}$$

$$\rho_0 \big[\partial_t(\mathbf{u}) + (\mathbf{u} \cdot \nabla)\mathbf{u} \big]$$
$$= -\nabla p + \eta \Big[\nabla^2 \mathbf{u} + \frac{1}{3} \nabla(\nabla \cdot \mathbf{u}) \Big] + \mu_0 \mathbf{M} \cdot \nabla \mathbf{H} - \rho \beta (T - T_0)\mathbf{g}, \tag{2.1b}$$

$$\Big[\rho_0 C_P - \mu_0 \mathbf{H} \cdot \Big(\frac{\partial \mathbf{M}}{\partial T} \Big)_H \Big] (\partial_t T + \mathbf{u} \cdot \nabla T)$$
$$= \lambda \nabla^2 T - \Big(\mu_0 T \Big(\frac{\partial \mathbf{M}}{\partial T} \Big)_H \cdot \frac{D\mathbf{H}}{Dt} \Big) \quad \text{(Fluid)}, \tag{2.1c}$$

$$\rho_H C_{PS} \partial_t T = \lambda_S \nabla^2 T \quad \text{(solid media)}, \tag{2.1d}$$

$$\Big(1 + \frac{M}{H} \Big) \nabla^2 \phi - \nabla \Big(\frac{M}{H} \Big) \cdot \nabla \phi = 0, \tag{2.1e}$$

where ρ_0 is the constant density, $\mathbf{u}$ is the velocity, p is the pressure, and T is the temperature; η is the dynamical viscosity, μ_0 is the magnetic permeability of vacuum, β is the expansion coefficient under the Boussinesq approximation, $\mathbf{H}$ is the magnetic field intensity and H its modulus, $\mathbf{M}$ is the magnetization and

$$M = \chi_0 \Big(1 - \frac{T - T_0}{T_c - T_0} \Big),$$

its modulus with T_0 and T_c being respectively the reference and the Curie temperatures and χ_0 the magnetization rate at T_0; ϕ is the scalar potential (with $\nabla \phi = \mathbf{H}$ for the non-conductive magnetic fluid), λ and λ_S are respectively the coefficients of thermal conductivity of the fluid and the solid media, C_p and C_{PS} being their respective specific heats at constant pressure.

In terms of lattice Boltzmann theory, Eqs. (2.1a)-(2.1e) can be solved by using three distribution functions for velocity, thermal and magnetic field [15] respectively f_α, g_α and h_α with:

$$f_\alpha(\mathbf{r} + \xi_\alpha \delta_t, t + \delta_t) - f_\alpha(\mathbf{r}, t) = -\frac{f_\alpha(\mathbf{r}, t) - f_\alpha^{eq}(\mathbf{r}, t)}{\tau_f} + \frac{(\tau_f - 0.5)\delta_t F \cdot (\xi_\alpha - \mathbf{u})}{\tau_f c_s^2} f_\alpha^{eq}, \tag{2.2a}$$

$$g_\alpha(\mathbf{r} + \xi_\alpha \delta_t, t + \delta_t) - g_\alpha(\mathbf{r}, t) = -\frac{g_\alpha(\mathbf{r}, t) - g_\alpha^{eq}(\mathbf{r}, t)}{\tau_g} + w_\alpha S \delta_t, \tag{2.2b}$$

$$h_\alpha(\mathbf{r} + \xi_\alpha \delta_t, t + \delta_t) - h_\alpha(\mathbf{r}, t) = -\frac{h_\alpha(\mathbf{r}, t) - h_\alpha^{eq}(\mathbf{r}, t)}{\tau_h}. \tag{2.2c}$$

The equilibrium distribution functions are given as:

$$f_\alpha^{eq}(\mathbf{r}, t) = w_\alpha \Big\{ \rho + \rho_0 \Big[\frac{\xi_\alpha \cdot \mathbf{u}}{c_s^2} + \frac{1}{2c_s^2} \Big(\frac{(\xi_\alpha \cdot \mathbf{u})^2}{c_s^2} - \mathbf{u}^2 \Big) \Big] \Big\}, \tag{2.3a}$$

$$g_\alpha^{eq}(\mathbf{r}, t) = w_\alpha T \Big\{ 1 + \frac{\xi_\alpha \cdot \mathbf{u}}{c_s^2} + \frac{1}{2c_s^2} \Big(\frac{(\xi_\alpha \cdot \mathbf{u})^2}{c_s^2} - \mathbf{u}^2 \Big) \Big\}, \tag{2.3b}$$

$$h_\alpha^{eq}(\mathbf{r}, t) = w_\alpha \phi \Big\{ 1 + \frac{\xi_\alpha \cdot \gamma \mathbf{u}_T}{c_s^2} + \frac{1}{2c_s^2} \Big(\frac{(\xi_\alpha \cdot \gamma \mathbf{u}_T)^2}{c_s^2} - (\gamma \mathbf{u}_T)^2 \Big) \Big\}. \tag{2.3c}$$

The force and source term are respectively:

$$\mathbf{F} = \mu_o M \nabla H - \rho_0 \beta (T - T_0) \mathbf{g}, \tag{2.4a}$$

$$S = -\frac{\mu_0 T \mathbf{M} \cdot \dfrac{D\mathbf{H}}{Dt}}{\left[\rho_0 C_P - \mu_0 \mathbf{H} \cdot \left(\dfrac{\partial \mathbf{M}}{\partial T}\right)_H\right]}. \tag{2.4b}$$

Here $\mathbf{r} = \mathbf{r}(x,y,z)$ is the spatial vector, $\mathbf{u}_T = -\nabla(M/H)$ is an effective velocity, γ is an adjustable preconditioning parameter introduced to ensure that the solution of the LB scheme (2.2c) remains close to a solution of the original scalar potential equation (2.1e). The relaxation parameters in Eqs. (2.2a)-(2.2c) are given by:

$$\tau_f = \frac{\eta}{\rho_0 c_s^2 \delta_t} + 0.5, \tag{2.5a}$$

$$\tau_g = \frac{D}{(D+2)} \frac{\lambda}{\left[\rho_0 C_P - \mu_0 \mathbf{H} \cdot \left(\dfrac{\partial \mathbf{M}}{\partial T}\right)_H\right] c_s^2 \delta_t} + 0.5, \tag{2.5b}$$

$$\tau_h = \frac{\gamma}{c_s^2 \delta_t} \left(1 + \frac{M}{H}\right) + 0.5, \tag{2.5c}$$

with D being the dimension of the problem. In numerical simulation, the value of the preconditioning parameter γ is chosen by setting τ_h close to 1 and avoiding the unphysical effects [16] due to the large value of $(1 + M/H)/\delta_t$.

The speed of sound c_s, the weight coefficient w_α and the discrete velocity ξ_α used in the above LBM equations are those from the D3Q19 discrete velocity model for 3-dimensional simulations [17]. The density, velocity, and temperature are then obtained by calculating the sum of the distribution functions over all the discrete directions α:

$$\rho = \sum_\alpha f_\alpha, \qquad \rho_0 \mathbf{u} = \sum_\alpha f_\alpha \xi_\alpha + 0.5 \delta_t \mathbf{F}, \tag{2.6a}$$

$$T = \sum_\alpha g_\alpha, \qquad \phi = \sum_\alpha h_\alpha. \tag{2.6b}$$

A number of previous researches [15] have shown that the macroscopic equations (2.1a)-(2.1e) can be deduced from the lattice Boltzmann equations (2.2a)-(2.2c) by the Chapman-Enskog analysis.

2.2 Numerical implementation and boundary conditions

To study the porous media case, we used the LBM to simulate the flow of the TSMF. The simulations set up a rigid cubic cavity of length $L = 8$mm with different number of obstacles modeled evenly placed acrylic balls. Temperatures of the bottom and upper walls are fixed at respectively T_b and $T_u = T_0 = 295.15$K. Other properties and values used in the simulation are summed up in Table 1. In the cavity, the temperature-sensitive magnetic fluid was submitted to a uniform vertical upwards magnetic field and a temperature difference

$$\Delta T_{ref} = T_u - T_b,$$

Table 1: Cavity dimension, fluid properties used in present study.

Scale length of cavity L(mm)	8	Specific heat C_p (J/kg·K)	1.39×10^3
Density ρ_0 (kg/m^3)	1.397×10^3	Expansion coefficient β (1/K)	6.90×10^{-4}
Viscosity η (Pa·s)	1.680×10^{-2}	Curie temperature T_c (K)	477.35
Thermal conductivity λ (W/(m·K))	1.750×10^{-1}	Reference temperature T_0 (K)	298.15
Thermal conductivity λ_S (W/(m·K))	1.11×10^2	Magnetization rate χ_0	0.2650
Permeability of vacuum μ_0 (H/m)	$4\pi \times 10^{-7}$	Gravitational acceleration g (m/s^2)	9.8
Density ρ_S (kg/m^3)	8.52×10^3	Specific heat C_{PS} (J/kg·K)	3.85×10^2

is applied, where the bottom wall is the hottest.

The purpose of the simulation is to study the influence of the number of obstacles (Fig. 1) as well as the effect of different values of the magnetic field. To parameterize the simulation, we used the Rayleigh number Ra and the magnetic Rayleigh number *Ram* given by:

$$Ra = \frac{\rho_0^2 g \beta \Delta T_{ref} L^3 C_p}{\eta_0 \lambda}, \qquad Ram = \frac{\rho_0^2 \mu_0 \chi_0 H_0^2 L^2 \Delta T_{ref} C_p}{\eta_0 \lambda}. \qquad (2.7)$$

As a result, we calculated the effective Nusselt number Nu to characterize the effectiveness of the heat transfer in the cell. We first carried investigations to ensure the grid-independence of the simulation over grids of size $21 \times 21 \times 21$ and $41 \times 41 \times 41$ before setting the number of Lattice-Boltzmann nodes to $31 \times 31 \times 31$ in all the following simulations. The study is carried for 1, 8 and 64 balls, as shown by Fig. 1; the porosity is kept constant at 0.477. In all the simulations the Rayleigh number was set to 40000 and the study was carried for three different values of the magnetic Rayleigh number: 0 (no magnetic field), 1.0×10^7 and 1.25×10^7. All results are calculated in non-dimensional forms by using scaled parameters of $\mathbf{r}/L$,

$$U_{ref} = \sqrt{g \beta L \Delta T_{ref}},$$

$T/\Delta T_{ref}$ and the preconditioning parameter is set as 5×10^{-3}.

The cavity walls are assumed to be non-slip. The side boundaries of the cell are adiabatic, and temperature is imposed at the top and at the bottom. The resulting boundary conditions of the macroscopic variables u and T are summed up in Fig. 2. Magnetic field is constrained by conditions over the magnetic potential ϕ:

$$\frac{\partial \phi}{\partial x}\bigg|_{x=0,L} = 0, \qquad \frac{\partial \phi}{\partial y}\bigg|_{y=0,L} = 0, \qquad \frac{\partial \phi}{\partial z}\bigg|_{z=0,L} = H. \qquad (2.8)$$

In the simulation, the temperatures on the isolated walls and the scalar potentials on all walls are calculated with a second-order extrapolation scheme. For distribution functions f_α, g_α and h_α on the boundaries, the non-equilibrium bounce-back boundary conditions [15] are used:

$$f_{\bar{\alpha}}(\mathbf{r},t) - f_{\bar{\alpha}}^{eq}(\mathbf{r},t) = f_\alpha(\mathbf{r},t) - f_\alpha^{eq}(\mathbf{r},t), \qquad (2.9a)$$

$$g_{\bar{\alpha}}(\mathbf{r},t) - g_{\bar{\alpha}}^{eq}(\mathbf{r},t) = -\left[g_\alpha(\mathbf{r},t) - g_\alpha^{eq}(\mathbf{r},t)\right], \qquad (2.9b)$$

$$h_{\bar{\alpha}}(\mathbf{r},t) - h_{\bar{\alpha}}^{eq}(\mathbf{r},t) = -\left[h_\alpha(\mathbf{r},t) - h_\alpha^{eq}(\mathbf{r},t)\right], \qquad (2.9c)$$
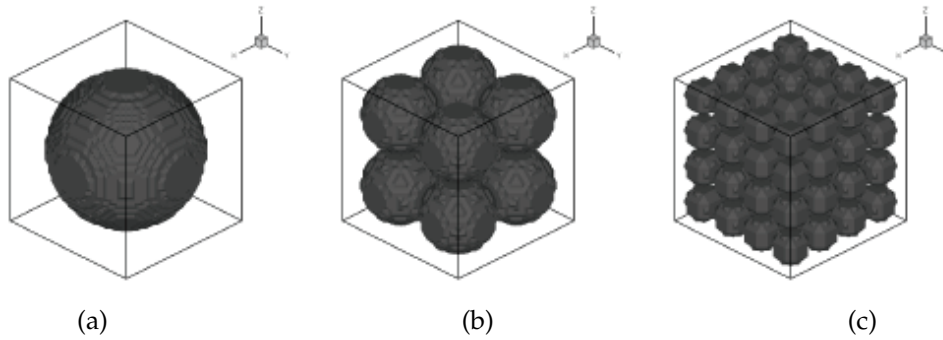
Figure 1: Porous media simulation cells: (a) 1 ball, (b) 8 balls, (c) 64 balls.

with $\overline{\alpha}$ being the opposite directions of the unknown distribution function.

3   Results and discussions

Fig. 3 shows the velocity vectors calculated by the simulation for the different cavities at the three values of the magnetic Rayleigh number. In Fig. 4 we plotted the temperature contour along with velocity vectors on two cross-sections for each case.

We can notice with these plots that the ball number has influence over the heat transfer capacity of the overall system. In fact, the more obstacles there are, the less the transfer seems to be efficient. In Fig. 3, the color of velocity vectors represents the temperature variation in the neighborhood. As the flow is more blocked when the ball number increases, it implies that the heat transfer efficiency decreases as the ball number increases. This can further be validated by Fig. 4, which displays the heat transportation inside the cavity enclosures with one ball ((a), (d), (g)), eight balls ((b), (e), (h)) and sixty-four balls ((c), (f), (i)). From this figure, we observe that the heat is trapped in bottom region when the numbers of ball increase. In fact, the more
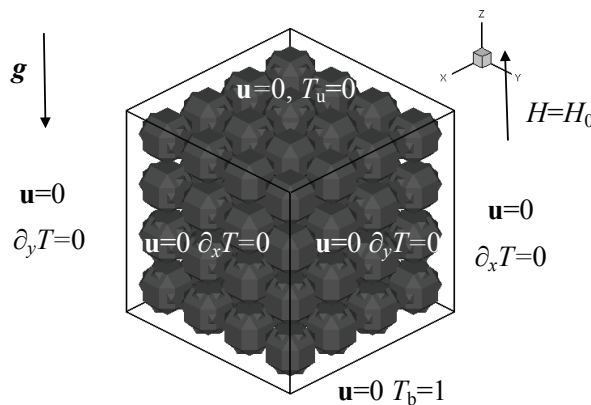

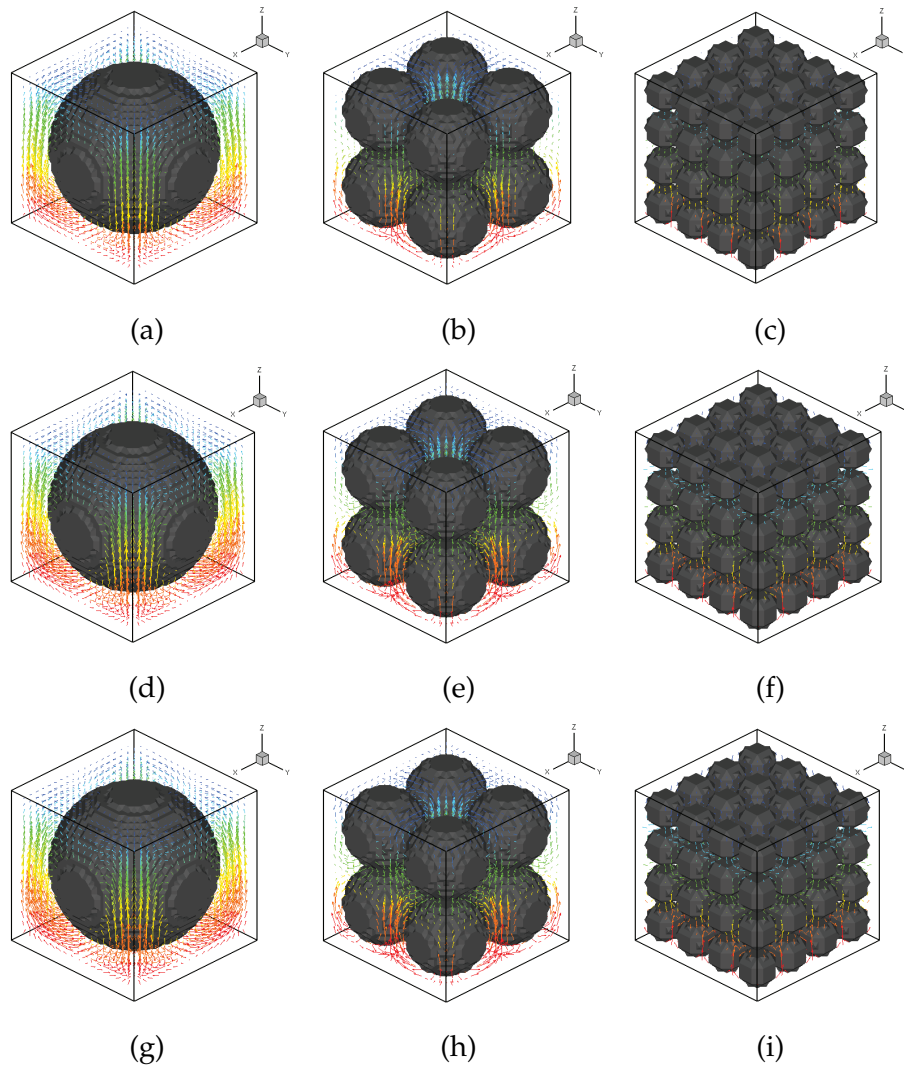Figure 2: Porous media simulation boundary conditions.

Figure 3: Velocity vectors for different magnetic Rayleigh numbers: (a)-(c) $Ram = 0$, (d)-(f) $Ram = 1.0 \times 10^7$, (g)-(i) $Ram = 1.25 \times 10^7$.

obstacles there are, the less the transfer is efficient. However the magnetic field also changes the heat transfer effectiveness, as we can see in Fig. 4. Increasing the magnetic field enhances the flow velocity in the pores, hence the better heat transportation.

To show clearly how the two effects interact, we will calculate the Nusselt number, an important parameter to measure the heat transfer of the materials. Here we will calculate the bulk Nusselt number in the whole domain and the average of the top or bottom wall Nusselt number.

$$Nu_a = \iint \left(-\frac{\partial T}{\partial Z} \right)\Big|_{z=0,L} dxdy, \qquad Nu_b = \iiint \left(-\frac{\partial T}{\partial Z} \right) dxdydz. \tag{3.1}$$

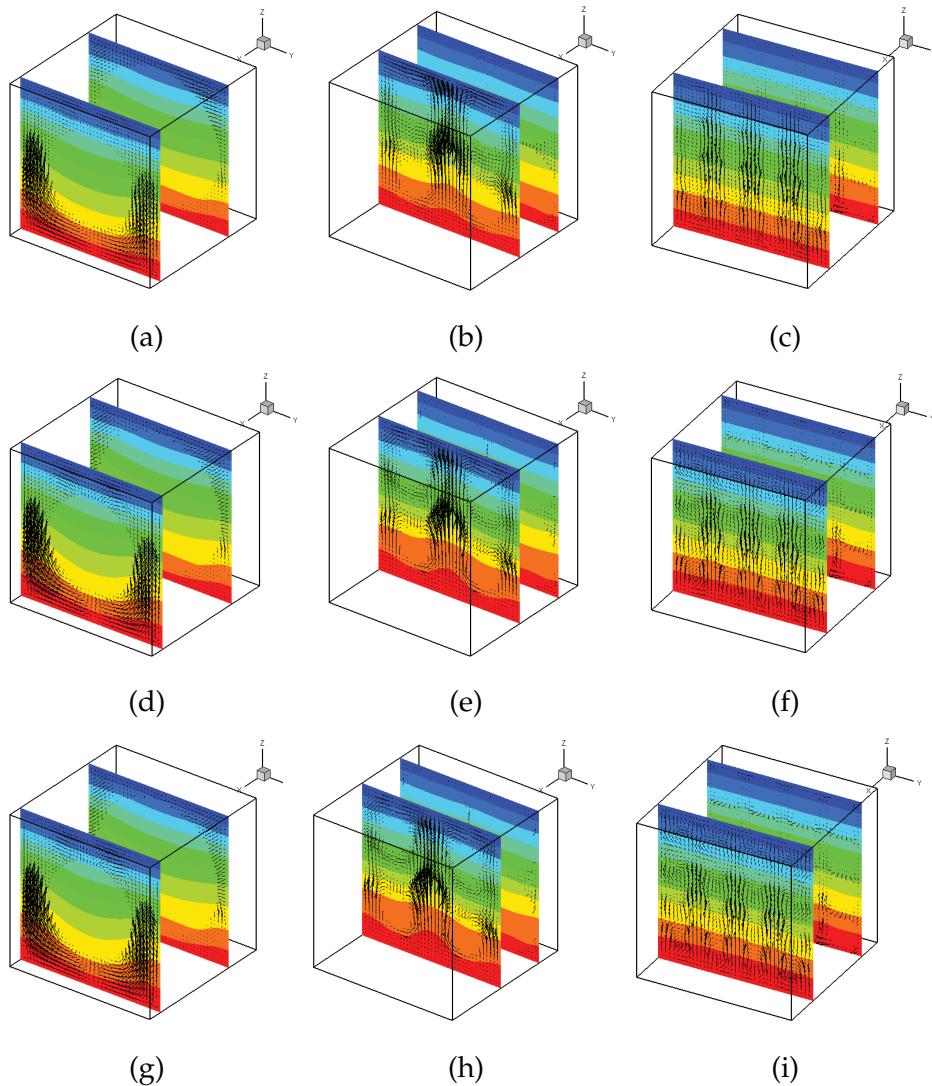The result has been plotted for the given simulations in Figs. 5 and 6.

Figure 4: Velocity vectors and temperature on two cross-sections for different magnetic Rayleigh numbers: (a)-(c) $Ram = 0$, (d)-(f) $Ram = 1.0 \times 10^7$, (g)-(i) $Ram = 1.25 \times 10^7$.

The first plot (Fig. 5) shows the effect of the number of balls and the magnetic field on the global heat transfer. As expected, increasing the number of balls makes the overall convective heat transfer decrease. Also, we see clearly that magnetic effects enhance the heat transfer, facilitating the flow in the cavity, hence the increase of the bulk Nusselt number in all cases when the magnetic Rayleigh number increases. On the other hand, we can notice in Fig. 6 that for small ball numbers (i.e., 1 and 8), the average wall Nusselt number increases with the magnetic Rayleigh number, while for high ball number, we observe a reverse effect: instead of increasing, the wall Nusselt number decreases when magnetic Rayleigh number increases, the flow being
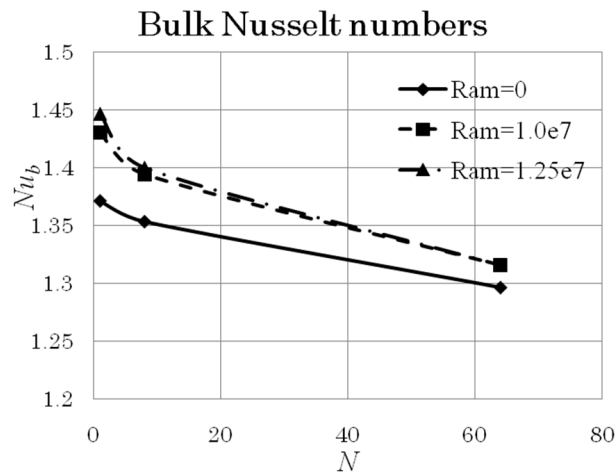
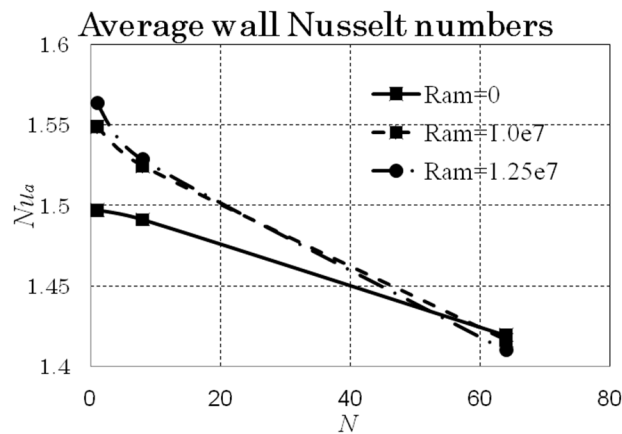Figure 5: Variation of bulk Nusselt number with ball numbers.

Figure 6: Variation of average Nusselt number with ball numbers.

"trapped" in the bottom (see Figs. 3(g)-(i) and 4(g)-(i)). With a large number of balls, the heat near the bottom is difficult to bring up due to the flow hindered by the balls.

4   Conclusions

A numerical simulation was performed to study the natural convective heat transfer problem of TSMF inside a porous medium-filled cubic enclosure under different magnetic fields. The porous media is represented by a number of evenly-placed balls in the cavity. Results show that the heat transfer decreases when the ball numbers increase. When the magnetic field is increased, the heat transfer is enhanced; however the average wall Nusselt number increases at small ball numbers but decreases at large ball numbers due to the flow being more likely confined near the bottom walls with a high number of obstacles.

Acknowledgements

References

[1] R. E. ROSENSWEIG, Ferrohydrodynamics, Cambridge University Press, London, 1985.

[2] H. YAMAGUCHI, Engineering Fluid Mechanics, Springer, Netherlands, 2008.

[3] R. HIEGEISTER, W. ANDRA, N. BUSKE, R. HERGT, I. HILGER, U. RICHTER, AND W. KAISER, *Application of magnetite ferrofluids for hyperthermia*, J. Magn. Magn. Mater., 201 (1999), pp. 420–422.

[4] S. SHUCHI, K. SASATANI, AND H. YAMAGUCHI, J. Magn. Magn. Mater., 289 (2005), pp. 257.

[5] B. M. BERKOVSKY, Magnetic Fluids Engineering Applications, Oxford University Press, New York, 1993.

[6] B. A. FINLAYSON, *Convective instability of ferromagnetic fluids*, J. Fluid. Mech., 40 (1970), pp. 753–767.

[7] L. SCHWAB, U. HILDEBRANDT, AND K. STIERSTADT, *Magnetic Bénard convection*, J. Magn. Magn. Mater., 39 (1983), pp. 113–114.

[8] M. S. KRAKOV, AND I. V. NIKIFOROV, *To the influence of uniform magnetic field on thermomagnetic convection in square cavity*, J. Magn. Magn. Mater., 252 (2002), pp. 209–211.

[9] H. YAMAGUCHI, I. KOBORI, Y. UEHATA, AND K. SHIMADA, *Natural convection of magnetic fluid in a rectangular box*, J. Magn. Magn. Mater., 201 (1999), pp. 264–167.

[10] H. YAMAGUCHI, I. KOBORI, AND Y. UEHATA, *Heat transfer in natural convection of magnetic fluids*, J. Thermophys. Heat. Transfer., 13 (1999), pp. 501–507.

[11] D. A. NIELD, AND A. BEJAN, Convection in Porous Media, third ed., Springer, New York, 2006.

[12] D. B. INGHAM, AND I. POP, Transport Phenomena in Porous Media, Elsevier, Oxford, 2005.

[13] S. CHEN, AND G. D. DOOLEN, *Lattice Boltzmann method for fluid flows*, Annu. Rev. Fluid. Mech., 30 (1998), pp. 329–364.

[14] M. S. KRAKOV, AND I. V. NIKIFOROV, *To the influence of uniform magnetic field on thermomagnetic convection in square cavity*, J. Magn. Magn. Mater., 252 (2002), pp. 209–211.

[15] X. D. NIU, H. YAMAGUCH, AND K. YOSHIKAWA, *Lattice Boltzmann model for simulating temperature-sensitive ferrofluids*, Phys. Rev. E., 79(4) (2009), 046713.

[16] P. LALLEMAND, AND L.-S. LUO, *Theory of the lattice Boltzmann method: dispersion, dissipation, isotropy, Galilean invariance, and stability*, Phys. Rev. E., 61 (2000), pp. 6546–6562.

[17] D. A. WOLF-GLADROW, Lattice-Gas Cellula Automata and Lattice Boltzmann Models, Springer, Berlin, 2000.